Determination of key operating conditions for the photocatalytic treatment of olive mill wastewaters

REFERENCE: E. Chatzisymeon, N.P. Xekoukoulotakis, D. Mantzavinos, Determination of key operating conditions for the photocatalytic treatment of olive mill wastewaters, *Catalysis Today* **144(1-2)** (2009) 143-148. http://dx.doi.org/10.1016/j.cattod.2009.01.037

Determination of key operating conditions for the photocatalytic treatment of olive mill wastewaters

Efthalia Chatzisymeon[♣], Nikolaos P. Xekoukoulotakis, Dionissios Mantzavinos*

Department of Environmental Engineering, Technical University of Crete, Polytechneioupolis, GR-73100 Chania, Greece

* Main corresponding author

E-mail: mantzavi@mred.tuc.gr; Tel: +30 28210 37797; Fax: +30 28210 37847

[♣] Second corresponding author

E-mail: thalia.chatzisymeon@gmail.com; Tel: +30 28210 37796; Fax: +30 28210 37847

Abstract

The TiO_2-mediated photocatalytic treatment of olive mill wastewater (OMW) was investigated in a batch type, laboratory scale photoreactor. UV-A irradiation was provided by a 400 W, high pressure mercury lamp and Degussa P25 TiO_2 was used as the catalyst. A factorial design approach was used to study the effect of various operating conditions such as initial organic loading, TiO_2 loading, pH, contact time and the addition of hydrogen peroxide on the conversion of COD and total phenols and experimental models describing the respective removals were developed. Effluent decolorization as well as process efficiency in terms of energy consumption were also evaluated. Finally, the acute ecotoxicity of OMW samples prior to and after photocatalytic treatment was assessed.

Keywords: olive mill wastewater, TiO_2 photocatalysis, factorial design, energy consumption

1. Introduction

The foodstuff processing industry based on olive oil extraction is an economically important activity for many regions of the Mediterranean Sea area. This process results in large quantities of bio-recalcitrant effluents that come from the vegetation water and the soft tissues of the olive fruits mixed with the water used at the different stages of oil production. All these wastewaters together with the industry washing waters make up the so called olive mill wastewater (OMW). Essentially, OMW consists of water (80–83%), organic compounds (15–18%) and inorganic compounds (2%), while the organic content varies broadly depending on many parameters such as the olive variety, harvesting time, climatic conditions and the oil extraction process. OMW also contains phytotoxic and biotoxic substances which prevent it from being disposed of. The phytotoxicity and strong antibacterial action have been attributed mainly to the polyphenolic content (0.5–24 g/L) found in OMW and secondarily to fatty acids present in olive oil residues [1]. The presence of these recalcitrant organic compounds constitutes one of the major obstacles in the detoxification of OMW.

Management of OMW and alike agro-industrial effluents is a complicated and pretty much unresolved issue with serious socio-economic implications. Given the unique characteristics of OMW (i.e. organic content of tens of g/L COD, seasonal and localized production involving small to medium size ventures), it is likely that a sequence of processes rather than a single operation may become the optimum treatment option. Such scheme could benefit from the integration of low-cost technologies (i.e. sedimentation, filtration, coagulation), conventional biological processes (i.e. aerobic and anaerobic) and the more costly advanced chemical oxidation to meet environmental regulations for discharge [2]. In recent years, advanced oxidation processes (AOPs) have been employed as alternative pretreatment methods aiming at reducing organic load and bio-recalcitrance of these effluents. Among them, photocatalytic methods have attracted a great deal of attention regarding OMW treatment. In a recent study, El Hajjouji et al. [3] studied the UV/TiO_2 treatment of OMW and found that oxidation for 24 h at 415 W intensity led to 94% phenols and 22% COD

removal respectively, while decolorization was 57%. Moreover, it was suggested that the compounds responsible for the persistent effluent COD after UV/TiO_2 attack were mainly pectins. In another recent study [4], the effect of various operating factors was investigated for the UV/H_2O_2/TiO_2 treatment of a synthetic solution containing 13 organic compounds typically found in OMW. OMW has also been treated by UV irradiation combined with other techniques such as ultrafiltration and ozonation [5, 6]. Reports on solar photocatalytic and photo-Fenton processes have also been published [7-9]. The possibility of reducing OMW phytotoxicity by means of solar irradiation combined with the Fenton reagent was investigated by Andreozzi et al. [7] and it was found that this process was not so efficient compared to other AOPs such as ozonation. On the other hand, the photo-Fenton process successfully removed 85% COD and up to 100% of phenolic compounds at a pilot-plant solar photoreactor [8].

The aim of this work was to study the photocatalytic oxidation of OMW regarding the effect of various operating conditions such as TiO_2 loading, initial organic loading, initial pH, contact time and the addition of hydrogen peroxide on the conversion of COD and total phenols (TPh). These parameters were chosen as they typically play a key role in dictating the performance of photocatalytic reactions. A factorial design methodology was adopted to determine in a systematic way the statistical significance of each parameter. Energy consumption of the process and ecotoxicity of OMW samples prior to and after treatment were also investigated.

2. Experimental and analytical

2.1. Materials

The OMW was provided by a three-phase olive oil mill company, located in Chania, Western Crete, Greece. The effluent was subjected to filtration to remove most of its total solids. The effluent has a strong olive oil smell and a dark black-brown color with maximum absorbance in the visible region at λ=550 nm. Its main properties prior to and after filtration are given in Table 1.

Degussa P25 TiO_2 was kindly supplied by Degussa AG (anatase:rutile 75:25, 21 nm primary crystallite particle size, 50 m^2/g BET surface area) and it was used as received. Hydrogen peroxide, as a 35% w/w solution, was supplied by Fluka.

2.2. Photocatalytic Experiments

UV-A irradiation was provided by a 400 W high pressure mercury lamp (Osram, HQL, MBF-U). The emission spectrum of the lamp consists of several spectral lines in the UV and visible region of which the main emission line exists at 366 nm [10]. Emission below 300 nm is impeded due to the reactor's material of construction (borosilicate glass). The photon flux emitted from the lamp was determined actinometrically using the potassium ferrioxalate method and was found to be $1.12\ 10^{-5}$ einstein/s.

Experiments were conducted in an immersion well, batch type, laboratory scale photoreactor described in detail elsewhere [11]. In a typical photocatalytic run, the original OMW was diluted with distilled water to achieve the desirable initial organic loading. Afterwards, 350 mL of the effluent were loaded in the reaction vessel and the solution was slurried with the appropriate amount of TiO_2. The resulting TiO_2 suspension was magnetically stirred for 30 min in the dark to ensure complete equilibration of adsorption/desorption of OMW organic compounds onto the catalyst surface which was about 10% in terms of COD. After that period of time, the lamp was turned on (this was taken as "time zero" for the reaction), while air was continuously sparged in the liquid and the reaction mixture was continuously stirred. Regarding the initial pH that took values of 4.8 (natural pH of the diluted effluent) and 7 (after adjustment with a few drops of 1 M NaOH solution), it should be noticed that the solution was not buffered to the aforementioned values. However, pH was monitored constantly throughout the reaction showing that only marginal changes had occurred between the initial and final solutions. In those cases where experiments were performed in the presence of hydrogen peroxide, the appropriate amount of 35% w/w solution of H_2O_2 was added to achieve the desirable final concentration of H_2O_2. All experiments were

conducted at constant temperature of 28±2°C. For each experimental run, 3 samples were taken, i.e. the first at the beginning of the experiment (time zero), the second after 1 hour of treatment and the third after 4 hours of treatment. The samples were filtered to remove solid particles and then analyzed for their residual COD, total phenolic content (TPh) and color.

Analytical measurements

COD was determined by the dichromate method. The appropriate amount of sample was introduced into commercially available digestion solution (0-1500 mg/L) containing potassium dichromate, sulfuric acid and mercuric sulfate (Hach Europe, Belgium) and the mixture was then incubated for 120 min at 150°C in a COD reactor (Model 45600-Hach Company, USA). COD concentration was measured colorimetrically using a DR/2010 spectrophotometer (Hach Company, USA).

The total phenolic content was determined colorimetrically at 765 nm on a Shimadzu UV 1240 spectrophotometer using the Folin-Ciocalteau reagent according to the procedures described in detail elsewhere [12]. Gallic acid monohydrate was used as standard to quantify the concentration of total phenols in OMW.

Sample absorbance was scanned in the 400-800 nm wavelength region on a Shimadzu UV 1240 spectrophotometer. Color was measured at λ=550 nm, which corresponds to the maximum absorbance in the visible region. Changes in sample absorbance at the wavelength of 550 nm were monitored to assess the extent of decolorization that had occurred during photocatalytic treatment.

H_2O_2 concentration in the OMW solution was monitored using Merck peroxide test strips (0-25 mg H_2O_2/L and 0-100 mg H_2O_2/L), while the pH was measured by a Toledo 225 pH meter during photocatalytic treatment.

The luminescent marine bacteria *V. fischeri* was used to assess the acute ecotoxicity of OMW samples. The inhibition of bioluminescense of *V. fischeri* was measured using a LUMIStox analyzer (Dr. Lange, Germany). Toxicity is expressed as EC_{50}, which is the effective concentration of a toxicant causing 50% reduction of light output during the designated time intervals at 15°C.

3. Results and discussion

3.1. Effect of operating parameters

In this work, a statistical approach was chosen based on a factorial experimental design that would allow us to infer about the effect of the variables with a relatively small number of experiments [13]. Five independent variables that may affect the photocatalytic treatment of OMW were taken into account, namely initial COD concentration, TiO_2 loading, solution pH, treatment time and H_2O_2 concentration. The experimental design followed in this work was a full 2^5 experimental set, which required 32 experiments. The order each experiment was performed was selected randomly. The design matrix of the experiments and the statistical analysis of these were made by means of the software package Minitab 14. The values chosen for the independent variables and the results obtained in terms of two measured response factors (dependent variables), namely concentration of COD oxidized in mg/L (response factor Y_1) and concentration of TPh removed in mg/L (response factor Y_2) are presented in Table 2. Table 2 also shows percent removal of COD, TPh and color.

Statistical treatment of the response factors Y_1 and Y_2 according to the factorial design technique involves the estimation of the average effect, the main effects of each individual variable as well as their two and higher order interaction effect [13]. The average effect is the mean value of each response factor, while the main and interaction effects are the difference between two averages: main effect= $\overline{Y_+} - \overline{Y_-}$, where $\overline{Y_+}$ and $\overline{Y_-}$ are the average response factors at the high and low level respectively of the independent variables or their interactions. Estimation of the average effect, as well as the main and interaction effects was made by means of the statistical package Minitab 14 and the results are summarized in Table 3.

A key element in the factorial design statistical procedure is the determination of the significance of the estimated effects. For the assessment of the significance of the main and interaction effects in un-replicated factorial designs, Minitab uses the Lenth's pseudo-standard error (PSE) [13, 14]. Lenth's PSE is an estimate of the standard error of the effects and for its calculation the median, m,

of the absolute values of the effects is first determined and then PSE=1.5 × m. Any estimated effect exceeding 2.5 × PSE is excluded and, if needed, m and PSE are recalculated. Then, a margin of error (ME) is given by ME= t × PSE, where t is the (1 - alpha/2) quantile of a t-distribution with degrees of freedom equal to the number of effects/3 [13, 14]. The present study was done for a confidence interval of 95%, therefore alpha=0.05. The calculated values of PSE and ME for the two response factors according to the Minitab software are also given in Table 3. All estimated effects greater than the ME can be considered significant. On the other hand, all other effects whose values are lower than the ME can be attributed to random statistical error.

A very useful pictorial presentation of the estimated effects and their statistical importance can be accomplished using the Pareto chart of the effects. The Pareto chart displays the absolute values of the effects in the ordinate, while a reference line is drawn at the margin of error, and any effect exceeding this reference line is potentially important. The Pareto charts of the effects for the COD and TPh oxidation are shown in Figs. 1 and 2 respectively.

As can be seen in Fig. 1, there are basically only two effects which are statistically important for COD oxidation, namely, in decreasing order of significance: the reaction time, and the initial concentration (influent) of COD. These effects are the most important factors affecting the oxidation of COD. The presence of oxidant, TiO_2 loading and the initial solution pH, along with all interactions, are not significant and may be explained as random noise. Both significant effects are positive indicating that an increase in their level brings about an increase in the amount of COD oxidized. The slightly positive (but still insignificant) effect of hydrogen peroxide on degradation may be due to the low H_2O_2:COD concentration ratio employed in this work, i.e. the additional oxidizing species generated by the dissociation of H_2O_2 lead to a measurable but marginal enhancement of degradation. In photocatalytic reactions, conversion invariably increases with increasing TiO_2 concentration up to a point above which it levels off; this corresponds to the point where all catalyst particles are fully illuminated. At higher concentrations, a screening effect of excess particles occurs, thus hindering light penetration; this usually results in conversion reaching

185 a plateau, while at excessive catalyst concentrations conversion may also decrease due to increased
186 light reflectance [4, 11]. It appears that the catalyst concentrations employed in this work fall within
187 this range, thus having a slightly negative but not statistically important influence on COD
188 conversion. A change in initial pH from 4.8 to 7 has no effect on conversion and this is consistent
189 with the results of Silva *et al* [4] who found that the photocatalytic treatment of a synthetic OMW in
190 the pH range 3.5-8 gave almost identical final conversions. It should be noticed here that the point
191 of zero charge of Degussa P25 TiO_2 is at pH=6.8; for the range of pH values in question, the
192 catalyst ionization state would remain unchanged (e.g. positively charged) and consequently would
193 not affect the degree of adsorption/reaction onto the surface.
194 Based on the variables which are statistically significant, a model describing the experimental
195 response Y_1 was constructed:
196
197 $$Y_1 = 601.75 + 184.5X_4 + 92X_1 \qquad (1)$$
198
199 where Y_1 is the mass of COD oxidized (mg/L), X_i are the transformed forms of the independent
200 variables according to:
201 $$X_i = \frac{Z_i - \left(\frac{Z_{high} + Z_{low}}{2}\right)}{\left(\frac{Z_{high} - Z_{low}}{2}\right)} \qquad (2)$$
202 and Z_i are the original (untransformed) values of the variables. The coefficients that appear in
203 equation (2) are half the calculated effects, since a change of X=-1 to X=1 is a change of two units
204 along the X axis.
205 The model predicts a linear dependency of the mass of COD oxidized on the operating variables.
206 Not only this, but it also indicates that the contact time (x_4) is the most significant variable in terms
207 of COD removal, because its effect has the highest value and its about two times greater than the
208 effect of influent organic loading (x_1). Therefore, the factorial design analysis shows that

photocatalytic treatment is more efficient, in terms of mass of pollutants removed, at increased organic loadings, thus implying that the concept of severe OMW dilution (usually with other industrial [15] or municipal wastewaters [16]) prior to treatment may be revisited. This undoubtedly enhances the use of TiO_2-mediated photocatalysis for OMW treatment.

Regarding TPh removal, the Pareto chart of the effects (Fig. 2) shows that contact time, influent COD and their interaction have a significant positive effect. On the other hand, the interactions of initial COD, TiO_2 and H_2O_2 loading as well as the interaction between TiO_2 loading and initial H_2O_2 concentration have a significant negative effect on TPh removal.

The following experimental model describes the TPh removal in mg/L:

$$Y_2 = 113.53 + 34.16X_4 + 30.91X_1 - 22.34X_1X_2X_5 - 18.97X_2X_5 + 15.91X_1X_4 \qquad (3)$$

It can be observed from eqn 3 that, contrary to eqn 1, the effect of the contact time is not much greater than the effect of the influent COD. Moreover, the effect of TiO_2 loading has an indirect negative effect on TPh removal through its interaction with initial COD and H_2O_2 concentrations. On the assumption that TPh are represented by gallic acid monohydrate, the stoichiometry of its reaction to carbon dioxide and water dictates that 100 mg of gallic acid would require 102 mg oxygen for the complete oxidation; therefore, Y_2 in Table 2 practically corresponds to the concentration of COD oxidized due to the phenolic fraction of the effluent. Comparison between Y_1 and Y_2 clearly shows that TiO_2 photocatalysis is a non-selective oxidation process, attacking simultaneously TPh and other organics.

In terms of color removal, decolorization mainly takes place during the first hour of treatment under almost all experimental conditions. As seen in Table 2, decolorization is always greater than 80%, and in most cases it is over 95%, at low influent COD; conversely, for influent COD of 5100 mg/L color removal typically varies between 40 and 70%. Interestingly, complete decolorization

coincides with equally high levels of TPh removal, thus implying that the OMW dark color is mainly due to the presence of phenolic compounds and their polymerized derivatives.

The validation of the mathematical model was based on the calculation of the residuals, which are the observed minus the predicted values according to the model, for the two response factors. The values of the calculated residuals for the two response factors were plotted in a normal probability plot and the results are shown in Figs. 3 and 4. For both responses, almost all data points lie close to a straight line and within the 95% confidence interval lines. These results indicate that the calculated residuals follow a normal distribution with mean values near zero. According to the above observations, it can be concluded that there is a good agreement between the experimental values and the mathematical model developed and the observed differences (i.e. the residuals) may be readily explained as random noise.

Eventually, the development of empirical mathematical models with relatively few experiments to describe OMW mineralization and TPh degradation is of great importance. Based on these models, an indicative view for scaling-up the process can be obtained.

Energy consumption

AOPs based on artificial light may be associated with increased operating costs, a major fraction of which is related to energy consumption. Bolton *et al* [17] introduced the concept of specific electric energy consumption per unit mass of pollutant (e.g. COD) degraded (E_{EM}):

$$E_{EM} = \frac{Pt}{V(COD_0 - COD)} \qquad (4)$$

where V is the effluent volume in liters, t is the treatment time in hours, P is the lamp power in kW, COD_0 and COD is the concentration in g/L before treatment and after time t respectively. Eqn (4) assumes that the reaction is zero-order with respect to COD, i.e. the removal rate is directly proportional to the rate of electric energy consumption. Although a thorough kinetic analysis was

outside the scope of this work, an attempt was made to evaluate the apparent order of reaction with respect to COD concentration based on the experimental data of Table 2. If the reaction were first-order, COD conversion would remain constant for runs performed at different initial COD values and all other variables being identical; conversely, for zero-order kinetics an increase in initial COD would result in a similar conversion decrease. In most cases (e.g. see runs 1 and 11, 2 and 12, 5 and 20, 6 and 22, 7 and 14, 9 and 19, 15 and 23, 26 and 32, 28 and 31), a 5-fold COD increase (i.e. from 1000 to 5100 mg/L) yields a decrease in the conversion by about 4-5 times, thus implying that the apparent reaction rate is near zero-order.

Applying eqn (4), it is evident that photocatalytic treatment is more efficient, in terms of energy consumption, at high influent COD values and short treatment times. For instance, comparing runs 29 and 17 energy consumption is 4.5 and 1.8 kWh/g COD removed after 1 h at 1000 and 5100 mg/L influent COD respectively; these values become 11 and 5 kWh/g COD removed after 4 h of treatment (runs 13 and 18). This fact comes to boost the conclusion, drawn from the factorial design analysis, that photocatalytic treatment is more efficient when working at increased organic loadings. Similar arguments can be inferred for TPh removal; energy consumption is 26.5 and 9 kW/g TPh removed after 1 h and 61 and 14.2 kW/g TPh removed after 4 h at 1000 and 5100 mg/L influent COD respectively (applying again eqn (4)). These values are seemingly greater than those for COD as the phenolic content comprises only a fraction of the total organic content.

Acute toxicity

The untreated effluent was highly ecotoxic to *V. fischeri* with an EC_{50} value of 12%. Changes in ecotoxicity were found to depend strongly on the residual organic matter following treatment. For instance at the conditions of run 23, the resulting effluent with a residual organic content of about 200 mg/L COD was non-toxic and this can be attributed to the complete removal of TPh. Conversely, when the experiment was performed at increased influent COD (run 15), the

285 ecotoxicity of the treated effluent remained nearly unchanged (EC_{50}=15%), thus indicating that the
286 residual 4150 mg/L COD (including about 200 mg/L TPh) contain various toxic species.
287
288 **4. Closing remarks**
289 Diluted wastewater from the olive oil industry was treated by TiO_2 photocatalysis with emphasis
290 given on the effect of various operating conditions on treatment efficiency with regard to COD and
291 TPh removal as well as decolorization. In order to evaluate the importance of the various
292 parameters involved in a coherent way, a factorial design methodology was followed. The
293 conclusions drawn from this study can be summarized as follows:
294
295 (1) COD removal was positively affected mostly by contact time and secondly by influent COD. All
296 other variables had no significant statistical importance to COD removal response. TPh removal
297 was positively affected by contact time and influent COD, while there was a negative effect through
298 the interaction of influent COD, TiO_2 and H_2O_2 concentrations.
299 (2) Simple, empirical models were developed and adequately simulated quantitatively the amount
300 of COD and TPh removed as a function of the most statistically significant effects for the range of
301 operating variables in question. These models may provide a useful tool for scaling-up and making
302 an economic analysis for an industrial application of the proposed process.
303 (3) Energy consumption per unit mass of pollutant removed is lower for high influent COD,
304 indicating that TiO_2 photocatalysis can be a promising process for OMW treatment.
305 (4) Monitoring ecotoxicity during photocatalytic treatment showed that OMW was almost
306 completely detoxified at low influent COD, while toxicity was only slightly reduced at increased
307 organic loadings.
308
309 **Acknowledgements**

310 This work is part of the 03ED391 research project, implemented within the framework of the
311 “Reinforcement Programme of Human Research Manpower” (PENED) and co-financed by
312 National and Community Funds (75% from E.U.-European Social Fund and 25% from the Greek
313 Ministry of Development-General Secretariat of Research and Technology).
314

315 **References**

316 [1] M. Niaounakis, C.P. Halvadakis, Olive-Mill Waste Management, 2nd Ed., Typothito, Athens,
317 Greece, 2006.
318 [2] D. Mantzavinos, N. Kalogerakis, Environ. Int. 31 (2005) 289.
319 [3] H. El Hajjouji, F. Barje, E. Pinelli, J.-R. Bailly, C. Richard, P. Winterton, J.-C. Revel, M.
320 Hafidi, Bioresource Technol. 99 (2008) 7264.
321 [4] A.M.T. Silva, E. Nouli, N.P. Xekoukoulotakis, D. Mantzavinos, Appl. Catal. B: Env. 73 (2007)
322 11.
323 [5] M. Drouiche, V.L. Mignot, H. Lounici, D. Belhocine, H. Grib, A. Pauss, N. Mameri,
324 Desalination 169 (2004) 81.
325 [6] K. Kestioglu, T. Yonar, N. Azbar, Process Biochem. 40 (2005) 2409.
326 [7] R. Andreozzi, M. Canterino, I. Di Somma, R.L. Giudice, R. Marotta, G. Pinto, A. Pollio, Water
327 Res. 42 (2008) 1684.
328 [8] W. Gernjak, M.J. Maldonado, S. Malato, J. Caceres, T. Krutzler, A. Glaser, R. Bauer, Sol.
329 Energy 77 (2004) 567.
330 [9] P.A.S.S. Marques, M.F. Rosa, F. Mendes, M.C. Pereira, J. Blanco, S. Malato, Desalinination
331 108 (1996) 213.
332 [10] T. Oppenländer, Photochemical Purification of Water and Air, Wiley–VCH, Weinheim,
333 Germany, 2003.
334 [11] E. Chatzisymeon, E. Stypas, S. Bousios, N.P. Xekoukoulotakis, D. Mantzavinos, J. Hazard.
335 Mater. 154 (2007) 1090.
336 [12] V. L. Singleton, R. Orthofer, R.M. Lamuela-Raventos, Methods Enzymol. 299 (1999) 152.
337 [13] G.E.P. Box, J.S. Hunter, W.G. Hunter, Statistics for experimenters: Design, Innovations, and
338 Discovery, 2nd ed., John Wiley & Sons, Inc., Hoboken, New Jersey, 2005.
339 [14] R.V. Lenth, Technometrics 31 (1989) 469.
340 [15] H.N. Gavala, I.V. Skiadas, G.Lyberatos, Water Sci. Technol. 40 (1999) 339.

341 [16] F.J. Rivas, F.J. Beltran, O. Gimeno, J. Frades, J. Agric. Food Chem. 49 (2001) 1873.

342 [17] J.R. Bolton, K.G. Bircher, W. Tumas, C.A. Tolman, Pure Appl. Chem. 73 (2001) 627.

343

344 **Table 1**. Properties of OMW samples used in this study.

Properties	Before filtration	After filtration
COD, g/L	47	40
Total phenols (TPh), g/L	8.1	3.5
Total solids, g/L	50.3	0.6
TOC, g/L	16.9	14
pH	4.6	4.4
Conductivity, mS/cm	17	18

345

346

Table 2. Design matrix of the 2^5 factorial experimental design and observed response factors (Y_1: mg of COD removed per liter; Y_2: mg of TPh removed per liter) as well as percent removal of COD, TPh and color.

Run order	X_1, $[COD]_0$, mg/L	X_2 $[TiO_2]$, g/L	X_3 pH	X_4 Reaction time, h	X_5 $[H_2O_2]$, mg/L	Y_1 COD oxidized, mg/L	Y_2 TPh oxidized, mg/L	% COD removal	% TPh removal	% Color removal
1	1000	2	7	1	500	286	72	29	77	95
2	1000	2	7	4	500	906	102	92	99	99
3	5100	0.5	7	1	0	790	49	15	11	9
4	1000	0.5	4.8	1	500	382	67	37	73	89
5	5100	0.5	7	1	500	400	144	8	27	38
6	5100	2	4.8	4	500	950	73	18	20	61
7	5100	0.5	7	4	0	860	155	17	34	28
8	5100	2	4.8	1	500	730	78	15	22	46
9	5100	2	7	1	0	370	66	7	12	18
10	5100	0.5	7	4	500	550	282	11	53	50
11	5100	2	7	1	500	390	78	8	19	63
12	5100	2	7	4	500	810	169	17	42	74
13	1000	2	4.8	4	0	412	75	42	85	93
14	1000	0.5	7	4	0	758	101	74	99	95
15	5100	0.5	4.8	4	500	950	205	19	43	58
16	1000	0.5	7	1	0	256	57	25	61	77
17	5100	2	4.8	1	0	630	125	12	24	39
18	5100	2	4.8	4	0	970	322	18	63	66
19	1000	2	7	1	0	254	67	25	55	76
20	1000	0.5	7	1	500	288	67	32	73	96
21	1000	0.5	7	4	500	820	109	91	99	99
22	1000	2	4.8	4	500	752	101	81	99	94
23	1000	0.5	4.8	4	500	798	104	78	99	93
24	1000	0.5	4.8	1	0	78	72	7	60	70
25	1000	2	4.8	1	500	360	70	39	71	82
26	1000	0.5	4.8	4	0	918	113	92	95	96
27	5100	0.5	4.8	1	500	660	126	13	27	47
28	5100	2	7	4	0	570	216	11	41	43
29	1000	2	4.8	1	0	252	43	26	49	64
30	5100	0.5	4.8	1	0	550	89	11	18	45
31	1000	2	7	4	0	636	102	62	85	97
32	5100	0.5	4.8	4	0	920	134	18	27	52

352 **Table 3.** Average and main effects of the independent variables and their two and higher order

353 interactions of the 2^5 factorial design on the response factors Y_1 and Y_2.

Effect	Value of Effect	
	COD removal	TPh removal
Average Effect	601.75	113.53
Main Effects		
x_1	184	61.81
x_2	-43.75	-7.19
x_3	-85.5	2.44
x_4	369	68.31
x_5	50.5	3.81
Two-factor Interactions		
$x_1 x_2$	11.25	0.06
$x_1 x_3$	-117	-1.56
$x_1 x_4$	-111.5	31.81
$x_1 x_5$	-78	-3.94
$x_2 x_3$	-18.75	-4.31
$x_2 x_4$	-27.25	1.81
$x_2 x_5$	85.75	-37.94
$x_3 x_4$	-9.5	11.19
$x_3 x_5$	-56	22.44
$x_4 x_5$	11	-12.94
Three-factor Interactions		
$x_1 x_2 x_3$	-63.75	-13.81
$x_1 x_2 x_4$	64.75	6.31
$x_1 x_2 x_5$	26.75	-44.69
$x_1 x_3 x_4$	-38.00	9.94
$x_1 x_3 x_5$	-26.50	24.44
$x_1 x_4 x_5$	1.50	-11.44
$x_2 x_3 x_4$	73.25	-4.81
$x_2 x_3 x_5$	60.25	4.19
$x_2 x_4 x_5$	60.30	-20.44
$x_3 x_4 x_5$	60.00	8.69
Four-factor Interactions		
$x_1 x_2 x_3 x_4$	-10.75	-4.06
$x_1 x_2 x_3 x_5$	67.25	14.19
$x_1 x_2 x_4 x_5$	-47.75	-20.44
$x_1 x_3 x_4 x_5$	2.50	8.94
$x_2 x_3 x_4 x_5$	-16.75	8.69
Five-factor Interactions		
$x_1 x_2 x_3 x_4 x_5$	39.25	9.44
Lenth's PSE	73.69	13.03
ME	163.5	28.91

354

355

356 **List of figures**

357

366

367

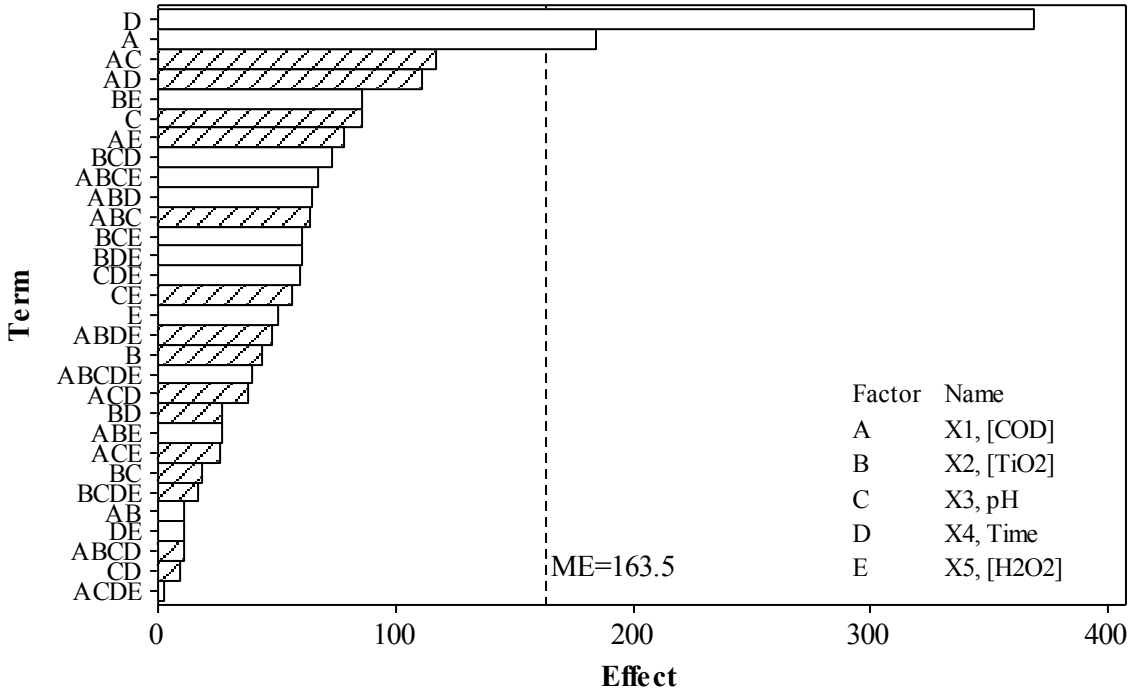

368

369 **Figure 1**

370

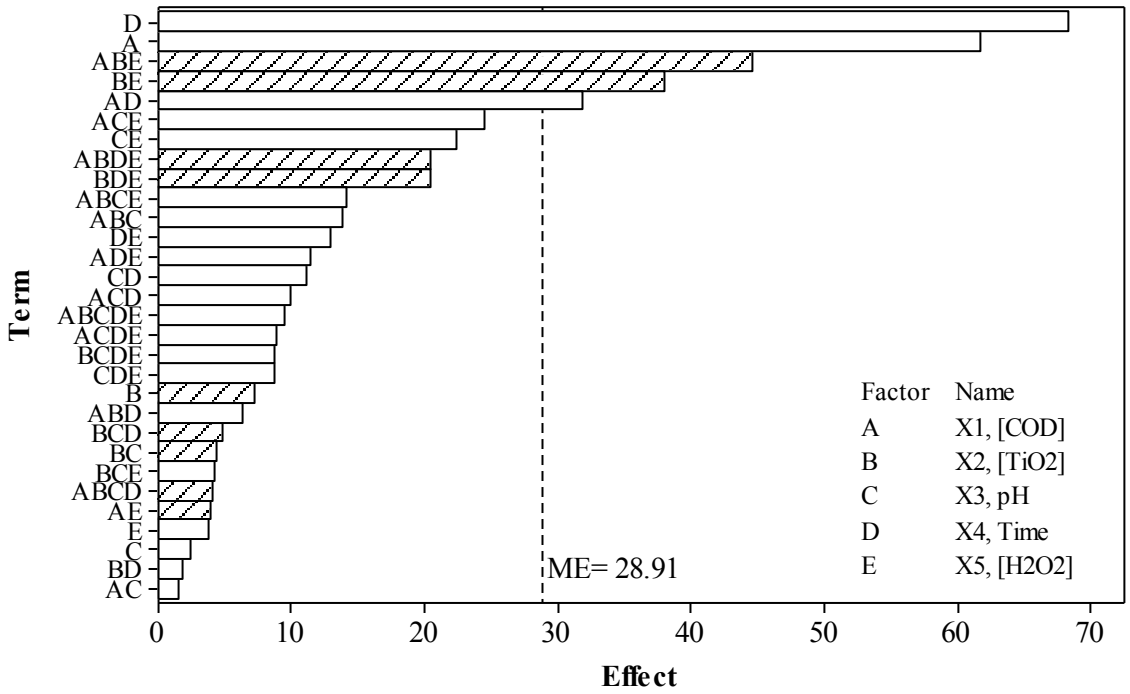

371

372 **Figure 2**

373

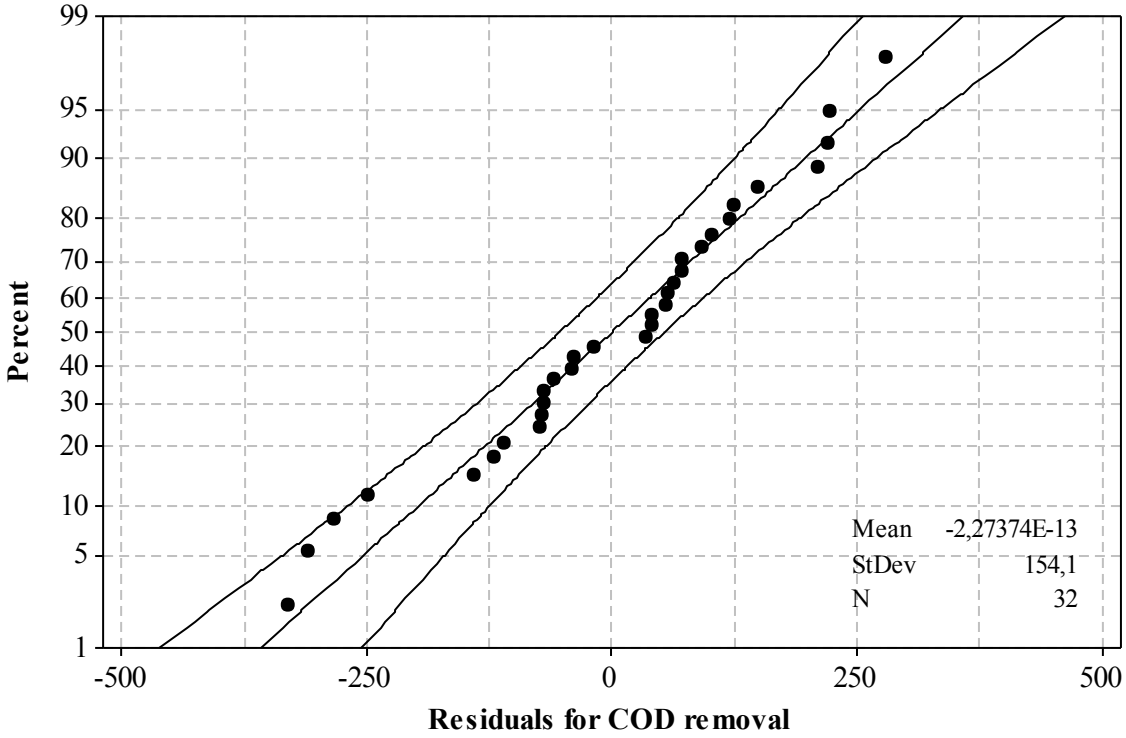

374

375 **Figure 3**

376

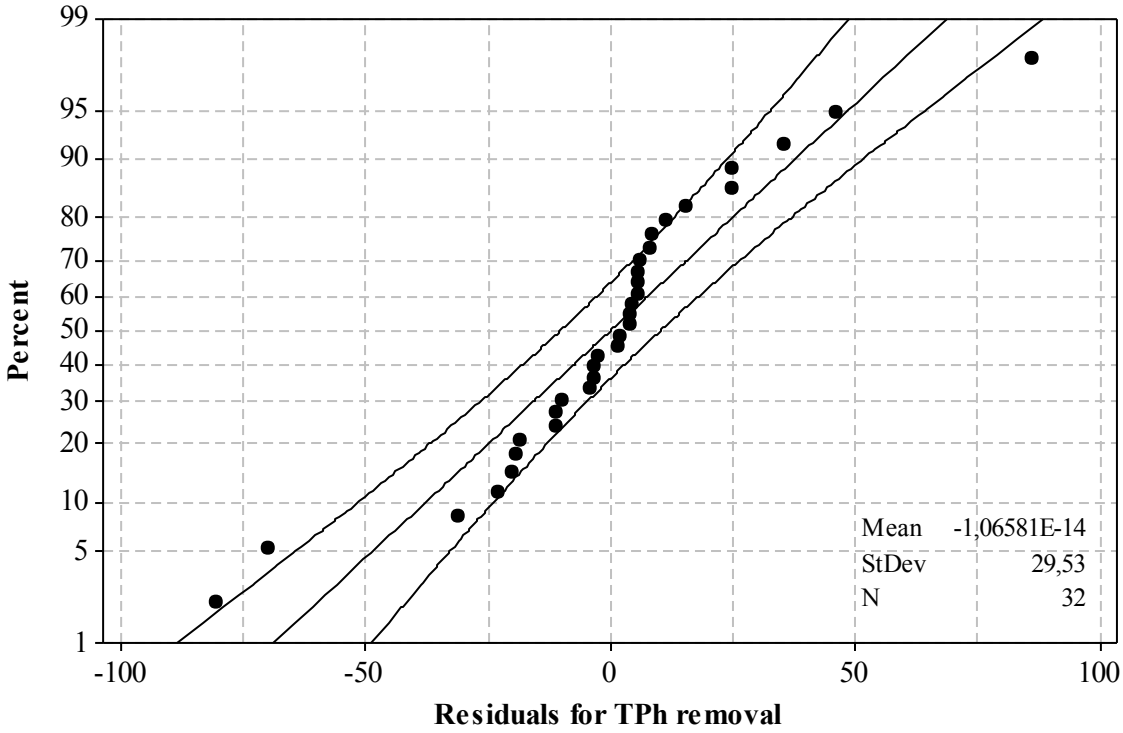

377

378 **Figure 4**